

RESEARCH ARTICLE

Cite this: *RSC Med. Chem.*, 2023, 14,
74Exploring structural effects in a new class of NRF2
inhibitors†Zhilin Hou,^a Lizbeth Lockwood,^b Di Zhang,^b Christopher J. Occhiuto,^b
Linqing Mo,^a Kelly E. Aldrich,^{‡a} Hayden E. Stoub,^c Kathleen A. Gallo,^c
Karen T. Liby^{*b} and Aaron L. Odom^{id *a}

NRF2 is a transcription factor that controls the cellular response to various stressors, such as reactive oxygen and nitrogen species. As such, it plays a key role in the suppression of carcinogenesis, but constitutive NRF2 expression in cancer cells leads to resistance to chemotherapeutics and promotes metastasis. As a result, inhibition of the NRF2 pathway is a target for new drugs, especially for use in conjunction with established chemotherapeutic agents like carboplatin and 5-fluorouracil. A new class of NRF2 inhibitors has been discovered with substituted nicotinonitriles, such as MSU38225. In this work, the effects on NRF2 inhibition with structural changes were explored. Through these studies, we identified a few compounds with as good or better activity than the initial hit but with greatly improved solubility. The syntheses involved a variety of metal-catalyzed reactions, including titanium multicomponent coupling reactions and various Pd and Cu coupling reactions. In addition to inhibiting NRF2 activity, these new compounds inhibited the proliferation and migration of lung cancer cells in which the NRF2 pathway is constitutively activated.

Received 5th July 2022,
Accepted 12th October 2022

DOI: 10.1039/d2md00211f

rsc.li/medchem

Introduction

NFE2-related factor 2 (NRF2) is a transcription factor that is activated by cellular stress to direct multiple responses to restore homeostasis. NRF2, and its negative regulator Kelch-like ECH-associated protein 1 (KEAP1), play a key role in the regulation of reactive species, such as hydrogen peroxide, reactive nitrogen species (*e.g.*, nitric oxide), and alkylating agents, in the cell.

Extensive evidence demonstrates that NRF2 activation suppresses carcinogenesis.^{1,2} Further, genetic deletion of NRF2 leads to a greater susceptibility to tumor formation.³

In cancer prevention studies, numerous compounds that activate the pathway are potential preventative drugs, many of which are found naturally in foods, such as isothiocyanate-containing sulforaphane found in broccoli and Brussels sprouts.⁴⁻⁷

However, constitutive NRF2 pathway activation in cancer cells reduces their sensitivity to chemo- and radiotherapy.² Loss-of-function mutations of *KEAP1* and gain-of-function mutations of *NFE2L2* (the gene that codes for NRF2) are found in many cancers. Mutations affecting this pathway (*NFE2L2*, *KEAP1*, *CUL3*, *BTRC*, and *MAFG*) are particularly prevalent in lung cancer cells with ~30% of all lung cancers containing such mutations. Consistent with these data, recent studies suggest that constitutive activation of the NRF2 pathway promotes tumor cell survival, proliferation, and metastasis.⁸⁻¹¹

Brusatol was the first NRF2 inhibitor to be identified and is still the most potent known;¹² however, profiling studies suggest that brusatol, rather than being a specific inhibitor, acts to inhibit global protein synthesis.¹³ Brusatol is also expensive to isolate or synthesize, which limits its potential clinical use. A few other small molecule inhibitors of NRF2 have been identified from screens, *e.g.*, AEM1,¹⁴ ML385,¹⁵ and IM3829.¹⁶ In addition, a few natural compounds,^{17,18} such as stigmaterol, have been shown to inhibit the pathway. In all cases, however, these inhibitors have lacked efficacy, selectivity or drug-like physical properties, and a review in

^a Department of Chemistry, Michigan State University, 578 S. Shaw Ln., East Lansing, Michigan 48824, USA. E-mail: odoma@msu.edu

^b Department of Pharmacology and Toxicology, Michigan State University, 1355 Bogue St., East Lansing, Michigan 48824, USA. E-mail: libykare@msu.edu

^c Department of Physiology, Michigan State University, 567 Wilson Rd., East Lansing, Michigan 48824, USA. E-mail: gallok@msu.edu

† Electronic supplementary information (ESI) available: Supplementary schemes for intermediates, synthetic details, characterization data for new compounds, data for kinetic studies related to ring closure, details for DFT studies, details for biological assays, representative purity analysis traces by GC/FID or HPLC, and ¹H/¹³C NMR spectra for new compounds. CCDC data for the X-ray diffraction study is available from the Cambridge Crystallographic Database under reference number 2091559. For ESI and crystallographic data in CIF or other electronic format see DOI: <https://doi.org/10.1039/d2md00211f>

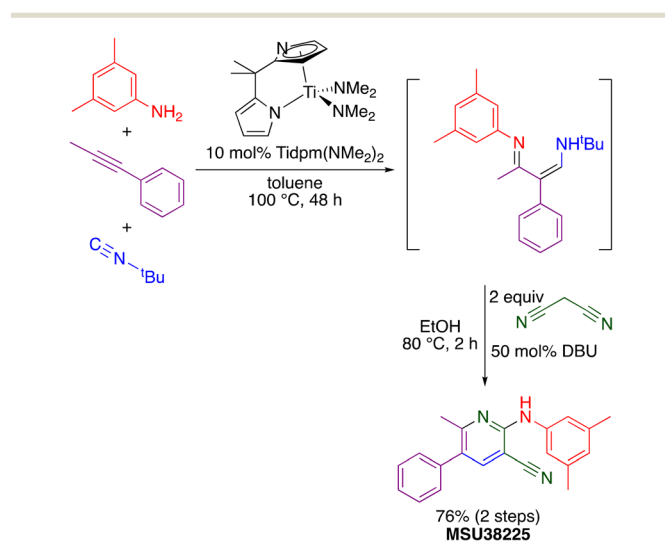
‡ Current address: Los Alamos National Laboratory, Los Alamos, New Mexico, 87545, U.S.A.

2019 declared NRF2 inhibitors a “completely open field for pharmacology”.¹⁹

In a recent publication, the Liby and Odom laboratories reported the discovery of a novel NRF2 pathway inhibitor, the small molecule MSU38225, which was effective *in vivo* and *in vitro*.²⁰ The compound showed promising selectivity for the NRF2 pathway and did not alter the concentrations of common off-target cellular proteins. Cells with constitutive NRF2-activity (*KEAP1* mutant) were more sensitive than wild-type cells to the compound. For example, MSU38225 inhibited proliferation of lung cancer cells with *KEAP1* mutations but did not affect normal epithelial cell growth. Importantly, the compound was found to act synergistically with chemotherapeutics like carboplatin (CI = 0.82) and 5-fluorouracil (CI = 0.54).

The “hit” compound MSU38225 was prepared using a novel titanium-catalyzed^{21–23} multicomponent coupling strategy in a one-pot procedure as shown in Scheme 1.²⁴ The Ti(dpm)(NMe₂)₂ (ref. 25)-catalyzed reaction, where dpm = deprotonated 5,5-dipyrrolylmethane, involves coupling of a primary amine, alkyne, and isonitrile, which forms both C–C and C–N bonds in the same catalytic cycle, alkyne iminoamination.²³ The product of the multicomponent coupling was not isolated but instead was treated with malononitrile and DBU to give a 2-aminonicotinonitrile.²⁴

In this work, NRF2-pathway inhibitory activity as a function of structure for this class of compounds was explored. The activity is quite sensitive to the structure of the inhibitor, and some compounds in the class can be activators rather than inhibitors with seemingly small chemical changes. In these, the first SAR studies on the class, changes were made around the core pyridine ring as well as a few changes to the central core. One major drawback of MSU38225 was its poor solubility, and, in addition to probing the effect of structure on activity, we were seeking a more soluble derivative with as good or better activity.



Scheme 1 Synthesis of MSU38225 using titanium-catalyzed multicomponent coupling in a one-pot procedure.

Results and discussion

The structural investigations were undertaken with a variety of goals, and the structure of MSU38225 was modified to determine (1) the functionality necessary for NRF2 inhibition, (2) where groups may be added to the structure without greatly affecting activity, (3) where heterocycles are tolerated, (4) what functional groups can be added to increase water solubility while retaining biological activity. We sought to increase or retain activity while improving water solubility to give a $\text{clog}P \leq 3$. To monitor NRF2 inhibition activities, a standardized luciferase assay with standard errors calculated based on multiple runs was employed.²⁰

To achieve these goals, a variety of different catalytic methods were brought to bear including titanium multicomponent, palladium, and copper coupling reactions. In some cases, further modifications were made, including protection/deprotection and hydrogenation. A few different core structures were investigated, but the focus was largely on changes to the periphery. Once the effects of substituents are better understood, the core may be further explored.

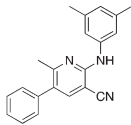
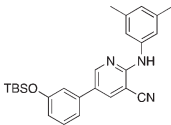
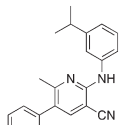
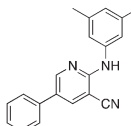
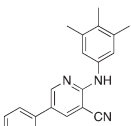
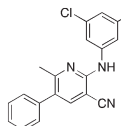
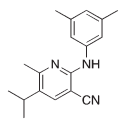
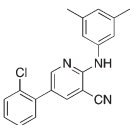
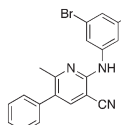
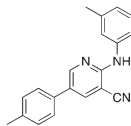
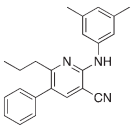
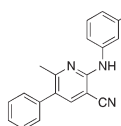
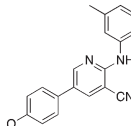
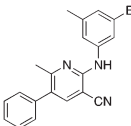
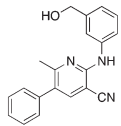
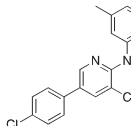
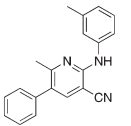
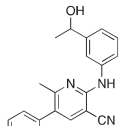
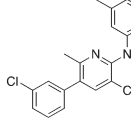
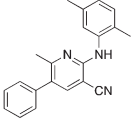
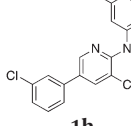
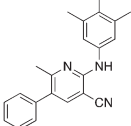
Synthesis of compounds and NRF2 inhibition assay results

The titanium-catalyzed chemistry shown in Scheme 1 was designed to allow rapid access to 2-aminonicotinonitriles in a one-pot procedure.²² As a result, it was further utilized here to produce derivatives of MSU38225 (**1a**), which was reprepared and tested for activity under identical conditions to the other compounds in this study. The initial hit **1a** and the other compounds prepared using this procedure are shown in Table 1.

The titanium chemistry tolerates many functional groups such as ethers, tertiary amines, secondary amines, halides, olefins, and others; however, the catalyst is sensitive to nitro groups, esters, amides, carboxylic acids, and alcohols. Alcohols, for example, may be protected using the typical procedures, such as silylation, which was employed for the synthesis of **1i**, **1u**, and **1v**. The yields were generally low for the derivatives described here, but the compounds were rapidly prepared using the one-pot procedure on scales more than adequate for biological testing and characterization, and the compounds were readily purified from the reaction mixtures.

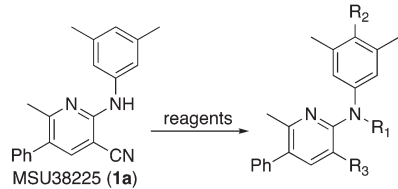
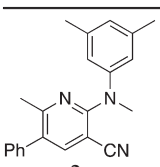
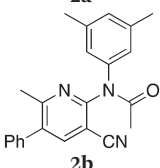
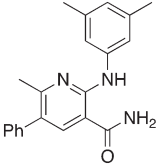
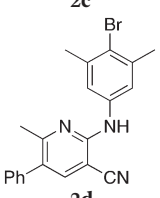
Titanium iminoamination was used to explore the effects of various aromatic groups on the 2-NH position (R¹, Table 1) by simply changing anilines, of which many are commercially available. In addition, the groups on the alkyne (R² and R³, Table 1) could be readily varied to explore the effects of these positions on activity. There is a strong tendency for sp²-carbons on the alkyne (vinyl or aromatic) to be placed in the 5-position of the pyridine during the synthesis; in fact, the other regioisomer is typically not observed in crude reaction mixtures by GC-MS. This was used to advantage in the synthesis of **1c**, where an enyne was used to direct the vinyl group to the 5-position followed by hydrogenation to the isopropyl group.

Table 1 Compounds prepared using titanium multicomponent coupling catalysis^a

Compound	ClogP ^b (solub.)	% yield (% activity)	Compound	ClogP ^b (solub.)	% yield (% activity)	Compound	ClogP ^b (solub.)	% yield (% activity)
 1a MSU38225	4.6 (3 μM)	34 (54.6 ± 2.1)	 1i	6.9	19 (12.6 ± 5.5)	 1q	5.1 (0.9 μM)	18 (55.2 ± 2.3)
 1b	4.4 (4 μM)	19 (38.4 ± 1.5)	 1j	4.8	14 (-32.3 ± 7.8)	 1r	5.1	28 (15.7 ± 1.8)
 1c	4.4	17, 35 ^c (-6.3 ± 13.6)	 1k	4.9	22 (32.9 ± 1.3)	 1s	5.4	19 (7.7 ± 4.7)
 1d	4.9	10 (-29.6 ± 4.1)	 1l	5.7	34 (-11.8 ± 18.1)	 1t	4.8	38 (51.8 ± 2.3)
 1e	4.4	12 (-1.5 ± 12.1)	 1m	5.0	19 (58.4 ± 6.2)	 1u	2.6	45, 56 ^d (16.7 ± 12.4)
 1f	5.2	17 (-4.9 ± 21.1)	 1n	4.1	29 (40.9 ± 5.2)	 1v	2.9	33, 54 ^d (26.0 ± 6) ^e (5.2 ± 7.5)
 1g	5.4	19 (49.2 ± 4.2)	 1o	4.6	15 (51 ± 2.6)			
 1h	5.2	23 (18.2 ± 12.9)	 1p	5.0	15 (37.2 ± 0.5)			

^a All compounds were purified to >98% purity by GC-FID. Yields are of purified compound after two synthetic steps, except as specified. Cellular activity where positive values indicate inhibition and negative values indicate activation. ^b ClogP calculated using ChemDraw 19.1 for the various structures. The experimental kinetic solubilities in μM were measured for a few derivatives. ^c Hydrogenation Yield. ^d Deprotection Yield. ^e Activity before deprotection.

Table 2 Derivatization of MSU38225 (**1a**)^a

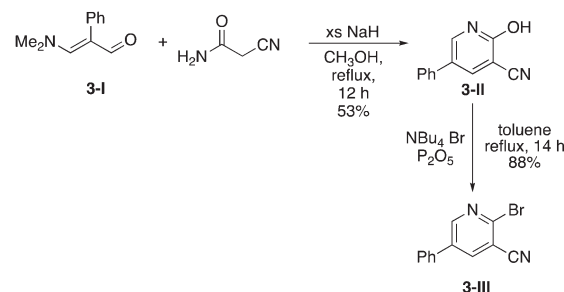
Compound	Reagents	Clog <i>P</i> ^b	% yield (% activity)
			
	KO ^t Bu, MeI	5.1	55 (21.9 ± 2.9)
	Ac ₂ O	3.1	69 (12.5 ± 8.7)
	{NBu ₄ } ⁺ OH ⁻ , EtOH	4.1	23 (-18.1 ± 8.9)
	NBS, (PhCO ₂) ₂	5.5	86 (25.7 ± 2.1)

^a All compounds were purified to >98% purity by GC-FID. Yields are of purified compound after two synthetic steps, except as specified. Cellular activity where positive values indicate inhibition and negative values indicate activation. ^b Clog *P* calculated using ChemDraw 19.1 for the various structures.

Several different methods of modifying MSU38225 (**1a**) were also investigated, and the activities of the resulting compounds were tested. These are shown in Table 2.

Methylation (**2a**) or acylation (**2b**) of the amine nitrogen substantially reduced activity. Base-catalyzed hydration of the nitrile to an amide resulted in a compound (**2c**) that was an NRF2 pathway activator (negative % activity), which could be an indication that hydrogen bonding donors/acceptors are important for the inhibition. Even simple bromination of the 4-position of the aromatic group to give **2d** lowered the biological activity compared to **1a**.

Due to the slow turnover frequency with heterocycle substrate in titanium-catalyzed iminoamination reactions, a different synthetic route was developed to expand the types of aromatic groups that would be added to the pyridine framework. We prepared 2-bromo-5-phenylnicotinonitrile **3-III** (Scheme 2) on multigram scales in a few steps. The first

**Scheme 2** Synthesis of 2-bromo-5-phenylnicotinonitrile (**3-III**).

step was a condensation involving 3-dimethylamino-2-phenylacrylaldehyde **3-I**, itself prepared by Vilsmeier–Haack formylation of phenylacetaldehyde dimethyl acetal. The aldehyde reacts with cyanoacetamide in the presence of base to give the 2-hydroxypyridine **3-II**. The conversion of the hydroxyl to bromo occurs in high yield with NBu₄⁺Br⁻ and P₂O₅.

The 2-bromo-5-phenylnicotinonitrile **3-III** in Scheme 2 was found to be a good substrate for Buchwald–Hartwig coupling with various aniline derivatives, as shown in Table 3. Of these compounds, of specific note is **3i**.§ All the compounds in Table 3 are closely related, e.g., **3f–3i** are isomers; as such, they have a clog *P* of ~2.5. However, **3i** is substantially more biologically active and shows good kinetic solubility. MSU38225 has a solubility of 3 μM in pH = 7.4 phosphate-buffered saline. The solubility of **3i** is 70 times greater at 209 μM. Once purified, it was obvious that **3i** exhibits two isomers in solution, and, to clarify, an X-ray diffraction study was undertaken. As shown in Fig. 1, the compound undergoes an intramolecular cyclization involving nucleophilic attack of one of the pyridine rings on the nitrile. This intramolecular cyclization was not observed on **3d** or **3f** due to methyl substitution adjacent to the pyridine nitrogen.

For **3i**, the closed form has a clog *P* of ~1.5, which suggests that the cyclized form is more water soluble compared to uncyclized form. When the compound is placed in solution, an equilibrium begins that takes ~36 h to reach completion in DMSO-*d*₆. The cyclized compound is favored in this polar medium with *K*_{eq} = 0.49 measured by ¹H NMR. The forward (*k*₁ = 1.5 × 10⁻⁵ s⁻¹) and back (*k*₋₁ = 3.0 × 10⁻⁵ s⁻¹) rate constants were also measured by fitting the ¹H NMR-derived concentrations as a function of time (see the ESI†).

In CDCl₃, the cyclized form is also favored with a *K*_{eq} = 0.77 (*k*₁ = 3.9 × 10⁻⁴ s⁻¹, *k*₋₁ = 5.1 × 10⁻⁴ s⁻¹); however, in less polar toluene the open form becomes favored with a *K*_{eq} = 1.48 (*k*₁ = 4.8 × 10⁻⁵ s⁻¹, *k*₋₁ = 3.3 × 10⁻⁵ s⁻¹). DFT calculations (B3PW91/cc-PVTZ) suggest that **3i** should favor the uncyclized species in a nonpolar environment as well (see the ESI†).

To explore the effect of moving the 5-phenyl group to the 4-position of the core pyridine, an alternative substrate for

§ Closely related, fluorinated **3i** has activity and solubility comparable to **3i** but hasn't seen as extensive study.

Table 3 MSU38225 derivatives prepared by Buchwald–Hartwig coupling^a

Compound	H ₂ NAr	ClogP ^b (solub.)	% yield	% activity
3a		-0.05	12	9.6 ± 0.2
3b		1.4	69	11.2 ± 5.8
3c		1.4	21	-33.9 ± 13.6
3d		2.9	50	20.0 ± 7.6
3e		0.95	35	13.2 ± 7.2
3f		2.4	63	-13.8 ± 5.5
3g		2.4	68	-20.3 ± 9.2
3h		2.4	68	25.3 ± 5.2
3i		2.4 1.5 ^c (209 μM)	42	46.7 ± 4.0
3j		2.9 2.1 ^c	30	42.3 ± 3.9
3k		1.9 0.9 ^c	62	39.7 ± 4.2
3l		2.8 1.9 ^c	77	55.3 ± 6.8
3m		2.9 2.0 ^c	22	-23.6 ± 7.8
3n		2.4 1.5 ^c	15	-0.1 ± 4.3
3o		3.7 2.8 ^c	82	43.3 ± 6.8
3p		1.4 0.6 ^c	23	-130.6 ± 33.4

Table 3 (continued)

Compound	H ₂ NAr	ClogP ^b (solub.)	% yield	% activity
3q		1.9 1.0 ^c	19	25.5 ± 11.8
3r		0.5 -0.5 ^c	40	28.3 ± 12.6

^a All compounds were purified to >98% purity by GC-FID. Yields are of purified compound after two synthetic steps, except as specified. Cellular activity where positive values indicate inhibition and negative values indicate activation. ^b ClogP calculated using ChemDraw 19.1 for the various structures. The experimental kinetic solubilities in μM were measured for a few derivatives. ^c ClogP value of cyclized form.

C–N bond coupling, commercially available 2-chloro-4-phenylnicotinonitrile, was utilized (Table 4). Testing of the 4-phenyl isomers of MSU38225 (**4a**) demonstrated that these compounds also display reasonable inhibition activity, although slightly less than their 5-phenyl analogs, *cf.*, **4a** (36.4%) vs. **1a** (51%) and **4c** (27.9%) vs. **3i** (46.7%). No intramolecular cyclization products were observed for **4d–f**, presumably due steric inhibition by phenyl adjacent to the nitrile.

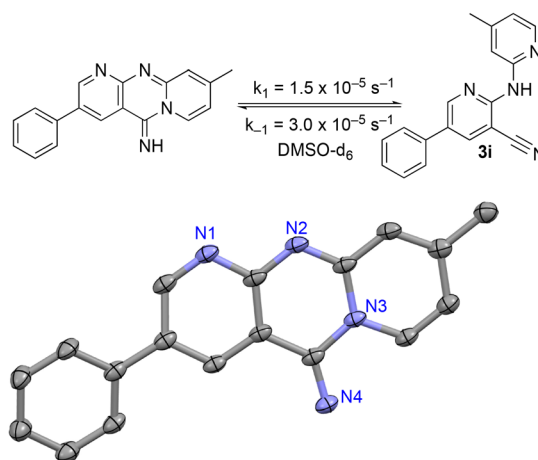
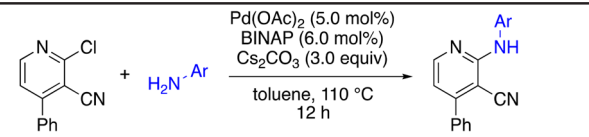
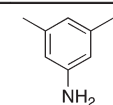
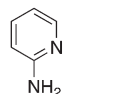
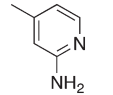
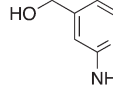
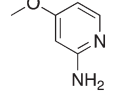
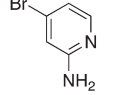
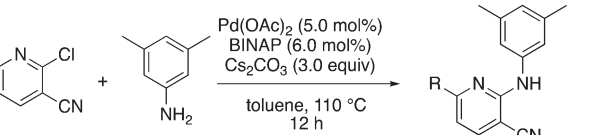


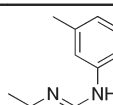
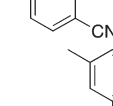
Fig. 1 Equilibrium between cyclized and uncyclized isomers for **3i**. The compound crystallizes as the cyclized species, which was characterized by single crystal X-ray diffraction and an ORTEP diagram (thermal ellipsoids = 50%) is shown. Hydrogens in calculated positions, a second chemically equivalent molecule in the asymmetric unit, and CH₂Cl₂ of crystallization are omitted. The rate constants in DMSO-d₆ were found by fitting the concentrations of both isomers versus an internal standard of ferrocene as functions of time by ¹H NMR spectroscopy (see the ESI†).

Table 4 Buchwald–Hartwig coupling to generate 4-phenylpyridine derivatives^a


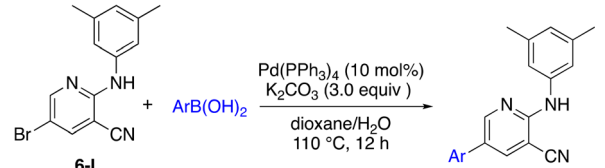
Compound	H ₂ NAr	Clog P ^b	% yield	% activity
4a		4.4	68	39.0 ± 4.4
4b		1.9	94	-78.1 ± 11.4
4c		2.4	73	35.4 ± 7.4
4d		1.4	74 75 ^c	-4.65 ± 5.5 ^d -31.77 ± 4.0
4e		1.9	87	-4.5 ± 1.8
4f		2.8	37	7.5 ± 5.1

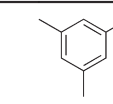
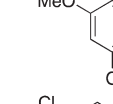
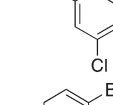
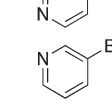
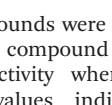
^a All compounds were purified to >98% purity by GC-FID. Yields are of purified compound after two synthetic steps, except as specified. Cellular activity where positive values indicate inhibition and negative values indicate activation. ^b Clog P calculated using ChemDraw 19.1 for the various structures. ^c Deprotection yield. ^d Activity before deprotection.

Table 5 Buchwald–Hartwig coupling to generate 6-substituted pyridine derivatives^a


Compound	Product	Clog P ^b	% yield	% activity
5a		3.1	56	6.1 ± 12.5
5b		4.7	95	3.7 ± 5.9

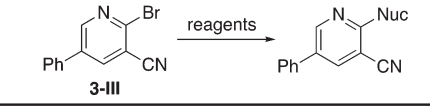
^a All compounds were purified to >98% purity by GC-FID. Yields are of purified compound after two synthetic steps, except as specified. Cellular activity where positive values indicate inhibition and negative values indicate activation. ^b Clog P calculated using ChemDraw 19.1 for the various structures.

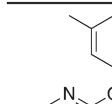
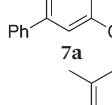
Table 6 Suzuki coupling reactions with 5-bromopyridines^a


Compound	ArB(OH) ₂	Clog P ^b	% yield	% activity
6a		5.4	74	25.1 ± 7.1
6b		4.3	84	-23.3 ± 2.7
6c		5.9	20	2.9 ± 2.4
6d		2.9	81	-42.8 ± 1.4
6e		2.9	79	-8.7 ± 4.4

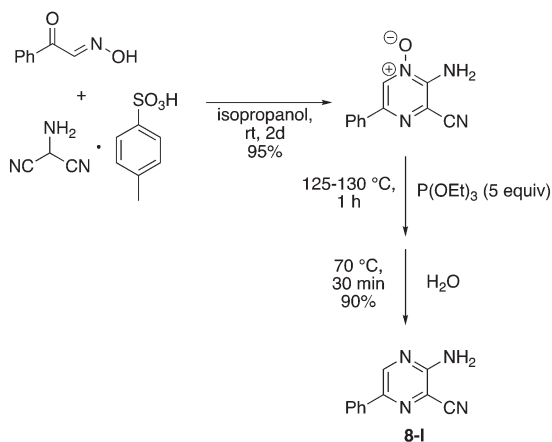
^a All compounds were purified to >98% purity by GC-FID. Yields are of purified compound after two synthetic steps, except as specified. Cellular activity where positive values indicate inhibition and negative values indicate activation. ^b Clog P calculated using ChemDraw 19.1 for the various structures.

Due to the strong tendency for sp²-carbons on the alkyne to be placed in the 5-position of the pyridine during the

Table 7 Replacements on 2-bromo-5-phenylnicotinonitrile to give O and CH₂ linkers^a


Compound	Clog P ^b	Reagents	% yield	% activity
	5.1	3,5-Dimethylphenol, NaH	58	-45.4 ± 10.4
	5.2	3,5-Dimethylbenzyl bromide, Zn dust	88	-33.9 ± 13.6

^a All compounds were purified to >98% purity by GC-FID. Yields are of purified compound after two synthetic steps, except as specified. Cellular activity where positive values indicate inhibition and negative values indicate activation. ^b Clog P calculated using ChemDraw 19.1 for the various structures.

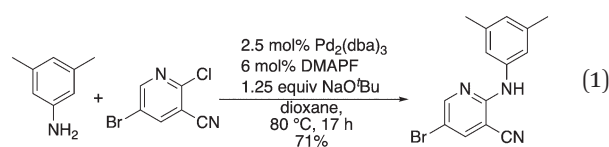


Scheme 3 Synthesis of 3-amino-6-phenylpyrazine-2-carbonitrile (**8-I**).

synthesis, Buchwald–Hartwig coupling was used to prepare **5b** (Table 5), the 6-phenyl derivative of active compound **1b**. For good measure, the 6-methyl derivative with no substituent on the 5-position was also prepared, which is MSU38225 (**1a**) sans 5-phenyl. These derivatizations extinguished the NRF2 inhibition activity observed in **1a** and **1b**.

A complementary synthetic route to titanium-catalyzed pyridine synthesis to incorporate heterocycles at the 5-position was developed using a selective chloride replacement at the 2-position of a pyridine in the presence of a 5-bromo group *via* Buchwald–Hartwig coupling using Pd₂(dba)₃ with DMAPF (eqn 1).²⁶ This left the 5-bromo-2-((3,5-dimethylphenyl)amino)nicotinonitrile (**6-I**), which is amenable to functionalization. Suzuki coupling utilized palladium(0) tetrakis(triphenylphosphine) with aqueous potassium carbonate in dioxane.²⁷ The reactions, generally, were high yielding using this synthetic protocol (Table 6); however, the substituted phenyl and pyridine compounds prepared in this class thus far have not exhibited NRF2 activity on par with **1a** or **3i**.

To further investigate the effect of the 2-position on activity, **1b** derivatives with bridging O and CH₂ linkers in place of NH (Table 7) were prepared. Replacement of the bromide in 2-bromo-5-phenylnicotinonitrile (**3-III**) occurs with simple nucleophiles. The O-linked compound was prepared by reaction with the sodium arylate, and the CH₂-bridged compound was accessed using BrZnCH₂(3,5-Me₂C₆H₃) prepared *in situ*. Both of these substitutions of the NH linker resulted in compounds that acted as NRF2 activators in the assay.



Finally, a few different cores in place of pyridine were explored. To increase solubility while maintaining a structure

Table 8 Chan–Lam coupling to generate pyrazine derivatives^a

Compound	Ar	ClogP ^b	% yield	% activity
8a	3,5-Me ₂ C ₆ H ₃	3.4	9	-7.8 ± 5.2
8b	3,5-(OMe) ₂ C ₆ H ₃	2.2	11	-66.0 ± 21.4

^a All compounds were purified to >98% purity by GC-FID. Yields are of purified compound after two synthetic steps, except as specified. Cellular activity where positive values indicate inhibition and negative values indicate activation. ^b ClogP calculated using ChemDraw 19.1 for the various structures.

very similar to MSU38225, we explored the use of pyrazines in place of the pyridine. A nearly ideal starting material, 2-amino-3-cyano-5-phenylpyrazine **8-I**, for making derivatives like **1b** can be synthesized with a 2-step synthesis (Scheme 3).²⁸ Chan–Lam coupling was used to install aromatic groups onto the NH₂-group in this starting material to make a compound that only differs from **1b** by having a nitrogen in the 4-position of the core in place of a CH (**8a**); interestingly, this compound showed no NRF2 inhibition activity. Placing a

Table 9 Synthesis of quinoline and 1,8-naphthyridine derivatives^a

Compound	ClogP ^b	% yield	% activity
9a	3.9	93	21.2 ± 13.8
9b	2.2	62	-9.5 ± 2.4
9c	2.4	30	-42.7 ± 16.6

^a All compounds were purified to >98% purity by GC-FID. Yields are of purified compound after two synthetic steps, except as specified. Cellular activity where positive values indicate inhibition and negative values indicate activation. ^b ClogP calculated using ChemDraw 19.1 for the various structures.

Table 10 Inhibition of A549 cell proliferation by novel NRF2 inhibitors

Compound	Structure	% inhibition ^a
1a (MSU38225)		9.8 ± 12.9
3i		59.8 ± 1.8
1m		35.3 ± 8.7
1t		26.6 ± 0.9

^a % inhibition of proliferation relative to standard. See ESI† for more details.

3,5-(OMe)₂C₆H₃ group on the 2-nitrogen gave a compound that activated the NRF2 pathway. The 2-NH₂ starting material (**8-I**) was also tested and found to be an NRF2 pathway activator, -25 ± 20% (Table 8).

In place of pyridine, quinoline and 1,8-naphthyridine were also briefly explored as core structures as shown in Table 9. The 2-amino starting materials were readily prepared using a Friedlander reaction between the 2-aminoarylaldehydes and malononitrile. Substituted aromatics were then installed onto the 2-amino group using Buchwald–Hartwig coupling catalyzed by Pd(OAc)₂ and XantPhos. However, these alternative cores were not inhibitors, and, in the case of **9b** and **9c**, are NRF2 activators.

Proliferation assay

Three of the more active compounds for inhibiting NRF2 pathway activation in the luciferase reporter assay were tested for their ability to inhibit proliferation of A549 human lung cancer cells. Cells were treated with 5 μmol L⁻¹ of compound for 72 h and viability was evaluated with an MTT assay. As shown in Table 10, all of these compounds inhibit proliferation of lung cancer cells, and **3i** was the most potent tested.

Expression of NRF2 and downstream targets results

To evaluate the impact of **3i** on NRF2 pathway signalling, NRF2 protein levels were assessed in non-small cell lung cancer cell lines with *KEAP1*-inactivating mutations that

promote constitutive NRF2 pathway activity. Consistent with previous results using MSU38225,²⁰ **3i** decreased NRF2 protein levels (Fig. 2A) to a similar extent as MSU38225 in A549 and H460 epithelial-like lung cancer cells (ATCC in Manassas, Virginia). Brusatol, a protein synthesis inhibitor and canonical inhibitor of the NRF2 pathway, was included as a positive control.²⁹ To demonstrate functional significance of **3i**-mediated NRF2 pathway downregulation, changes in NRF2 transcriptional activity in A549 cells were evaluated by measuring NRF2 target gene expression with RT-PCR. The mRNA levels of NQO1, GCLC, AKR1C2, and GCLM were significantly ($p < 0.001$) reduced by treatment with MSU38225 and **3i** (Fig. 2B).

Viability and cell cycle assays

Given the cytoprotective effects of NRF2 pathway activation, changes in viability of the lung cancer cells with constitutive NRF2 activity were analyzed using MTT assays. Compound **3i** decreased viability of A549 and H358 lung cancer cells in a dose-dependent manner with IC₅₀ values of 0.61 and 0.58 μmol L⁻¹, respectively, following 72 h of treatment (Fig. 2C). As determined by univariate cell cycle analysis, both MSU38225 and **3i**, but not brusatol, arrested A549 and H460 cells in the G2/M phase (Fig. 2D). These results highlight differences in the mode of action between **3i** and brusatol. Brusatol has been shown to globally inhibit protein synthesis.²⁹ In contrast, MSU38225 and **3i** have not been found to inhibit proteins unrelated to the NRF2 pathway.²⁰

Migration assay

Recently, an important role for NRF2 in lung cancer metastasis has emerged.^{10,30} To investigate the ability of NRF2 pathway inhibitors to block cancer cell migration, we used a transwell migration assay with 5% FBS as a chemoattractant. When A549 cells were treated with vehicle or 10 μmol L⁻¹ of MSU38225 and **3i**, migration was significantly ($p < 0.0001$) reduced by 65% and 80%, respectively (Fig. 2E). To determine the dose-dependence of the **3i** results, the transwell assay was repeated with vehicle or 1, 5, and 10 μmol L⁻¹ of **3i**. While 1 μmol L⁻¹ of **3i** was insufficient to alter A549 migration, 5 μmol L⁻¹ **3i** reduced migration by 72% and 10 μmol L⁻¹ **3i** reduced migration by 79% (Fig. 2F).

Conclusions

Our initial hit, MSU38225 (**1a**), is of low solubility and has modest (IC₅₀ ~ 5 μmol L⁻¹) activity, but it is a first-in-class NRF2 inhibitor with a structure amenable to synthetic investigation. Here, ~50 compounds with related structures were prepared to increase the activity and improve solubility. As noted, the activity is extremely sensitive to the

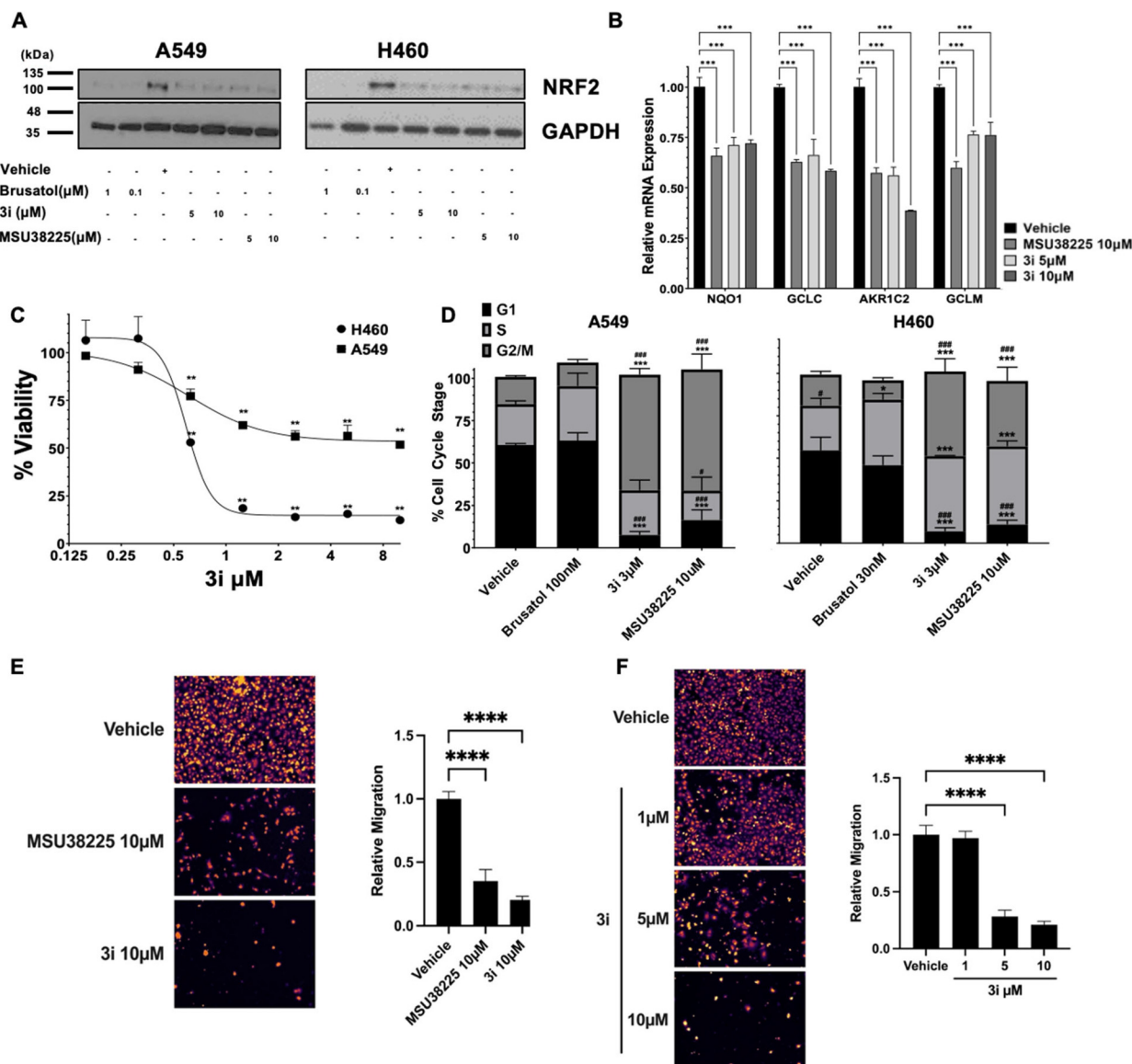


Fig. 2 Compound 3i inhibits expression of NRF2 target genes, reduces viability in lung cancer cells, and blocks migration. A549 or H460 cells were incubated for 24 h and (A) NRF2 protein levels or (B) mRNA expression in A549 cells were evaluated by western blotting or RT-PCR. NRF2 target genes were normalized to GAPDH and the DMSO vehicle control. Data are representative of 3 independent experiments. (C) Cells were treated for 72 h with various concentrations of 3i. Cell viability was measured using an MTT assay and values normalized as a percentage of vehicle (DMSO) control. $n = 3$ replicates. (D) Cells were synchronized in low serum media for 12 h, then treated for 24 h with inhibitors. Cell stage was analyzed by propidium iodide staining and flow cytometry, specifically univariate cell cycle analysis using a Watson pragmatic model with G0/1 and G2/M peak constraints ($n = 2-3$ independent experiments). Data are plotted as mean \pm SE percentage of total cells. A549 cells were seeded in serum-free medium containing (E) DMSO vehicle, 10 μM of NRF2 pathway inhibitors MSU38225 or 3i; or (F) DMSO vehicle, and the indicated doses of 3i in the top chamber of transwells. Media containing compounds and 5% FBS as a chemoattractant was used in the bottom chamber and cells were allowed to migrate for 24 h, at which point transwell filters were fixed and unmigrated cells were removed. The remaining cells were stained with DAPI, and imaged (9 fields per transwell insert, representative image shown). Two transwell inserts were used for each condition, $n = 2-3$ experimental replicates. Data were analyzed by one-way or two-way ANOVA. * = $p < 0.05$; ** = $p < 0.01$; *** = $p < 0.001$; **** = $p < 0.0001$ vs. vehicle control. # = $p < 0.05$; ### = $p < 0.001$ vs. brusatol.

structure (Fig. 3), which varies widely with small changes to some positions of the hit compound. Surprisingly, some of the newly synthesized compounds act as activators instead of inhibitors. In a series of experiments (Table 2), many simple modifications of 1a did not lead to improved activity, but the experiments give some insight into the features necessary for NRF2 inhibition by the class. In

particular, hydration of the nitrile to an amide removed the activity (2c).

Modifications of the 2-NH group were surveyed by replacing the hydrogen with a variety of groups such as Me (2a) and Ac (2b), which removed the inhibition activity. Similarly, replacing the NH with O (7a) or CH₂ (7b) gave NRF2 activators.

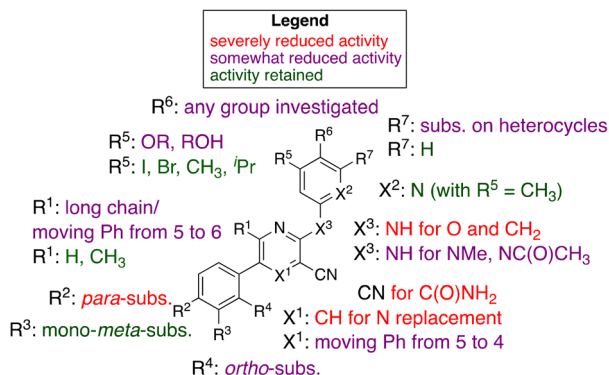


Fig. 3 Graphical summary of selected results.

While **1b** shows activity for NRF2 inhibition, in general, removal of the 6-methyl group from structures like **1a** did lower the activity, cf. **1g** and **1h**. However, lengthening the chain in this position to an *n*-Pr gave a compound with no activity (**1l**).

There is a 5-phenyl group in **1b** and moving the phenyl group to the unoccupied 4-position gave a compound with some activity (**4a**). This was seen in other compounds as well (**3i** vs. **4c**), where the 4-Ph was somewhat less active than if this group is in the 5-position. Placing the phenyl group in the 6-position extinguished the activity entirely, consistent with the activity of other compounds larger than methyl (e.g., **1l**).

Replacement of 5-phenyl with aromatics containing donor atoms and heterocycles can give potent activators. In fact, *para*-substitution does not seem to be well tolerated, but chloro and methyl can be added to *meta*-positions to get inhibitors.

Most core changes led to no activity or compounds that were activators. One exception is the switch from pyridine to quinoline (**1i**), which is promising.

Similarly promising results were found by replacing the groups on the 2-NH with various heterocycles. In particular, **3i** shows activity slightly higher than our initial hit (**1a**, MSU38225). The compound also demonstrates a reversible cyclization reaction (Fig. 1). Considering the nitrile seems to be important for activity (*vide supra*), it seems likely that the “open” form is what leads to the activity. This cyclization seems to be blocked by addition of a methyl group adjacent to the pyridine nitrogen (**3d**); however, this compound is inactive, muddling conclusions regarding the utility of the cyclization in the desired biological activity.

A very promising lead compound was found in **3i**, which reduces NRF2 protein levels and mRNA of downstream target genes, inhibits proliferation of lung cancer cells by inducing G2/M arrest, and suppresses invasion. Compound **3i** has markedly better anti-proliferative and anti-migratory activity (Fig. 2E) than MSU38225 (**1a**) and works through a different mechanism than brusatol (Fig. 2D). In addition, **3i** has a kinetic solubility ~70 higher (209 μ M) than **1a**. Further

studies on the activities of **3i** and related compounds and their anticancer activity *in vivo* are underway.

Abbreviations

DMAPF	1,1'-Bis(bis(dimethylamino)phosphino)ferrocene
Xantphos	4,5-Bis(diphenylphosphino)-9,9-dimethylxanthene
BINAP	(2,2'-Bis(diphenylphosphino)-1,1'-binaphthyl)
NBS	<i>N</i> -Bromosuccinimide
<i>m</i> CPBA	<i>meta</i> -Chloroperoxybenzoic acid
H2dpm	5,5-Dimethyldipyrrolylmethane
<i>t</i> BHQ	<i>tert</i> -Butylhydroquinone
MTT	3-(4,5-Dimethylthiazol-2-yl)-2,5-diphenyltetrazolium bromide

Conflicts of interest

A patent application has been submitted on the compounds in this article.

Acknowledgements

This work was supported by the National Science Foundation CHE-1953254 and MRI-1919565, MTRAC for Life Sciences Innovation Hub-Mi-Kickstart Award, a Molecular Discovery Group Pilot Grant from MSU, Discovery Funding Initiative (DFI) funding from MSU's Office of Research and Innovation, ACS-Petroleum Research Fund 65702-ND3, and NIH R01 grant (RC226690). Di Zhang was supported by the Integrative Pharmacology Sciences Training Program (IPSTP) training fellowship 5T32GM092715-07, a fellowship from the Aitch Foundation, a Penner Fund Fellowship, and a NIH NCI F99/K00 fellowship (CA245473). Kelly Aldrich was supported by a grant from the American Association of Women. Zhilin Hou was supported by a fellowship from Michigan State University. The authors thank Edmund Ellsworth for helpful discussion.

Notes and references

- S. Menegon, A. Columbano and S. Giordano, *Trends Mol. Med.*, 2016, **22**, 578–593.
- M. B. Sporn and K. T. Liby, *Nat. Rev. Cancer*, 2012, **12**, 564–571.
- T. O. Khor, M. T. Huang, A. Prawan, Y. Liu, X. P. Hao, S. W. Yu, W. K. L. Cheung, J. Y. Chan, B. S. Reddy, C. S. Yang and A. N. Kong, *Cancer Prev. Res.*, 2008, **1**, 187–191.
- A. T. Dinkova-Kostova, *Ann. Nutr. Metab.*, 2015, **67**, 14.
- A. T. Dinkova-Kostova, J. W. Fahey, R. V. Kostov and T. W. Kensler, *Trends Food Sci. Technol.*, 2017, **69**, 257–269.
- Y. Yagishita, J. W. Fahey, A. T. Dinkova-Kostova and T. W. Kensler, *Molecules*, 2019, **24**, 3593.
- H. Robertson, A. T. Dinkova-Kostova and J. D. Hayes, *Cancers*, 2020, **12**, 3609.

- 8 E. A. Collisson, J. D. Campbell, A. N. Brooks, A. H. Berger, W. Lee, J. Chmielecki, D. G. Beer, L. Cope, C. J. Creighton and L. Danilova, *et al.*, *Nature*, 2014, **511**, 543–550.
- 9 P. S. Hammerman, M. S. Lawrence, D. Voet, R. Jing, K. Cibulskis, A. Sivachenko, P. Stojanov, A. McKenna, E. S. Lander and S. Gabriel, *et al.*, *Nature*, 2012, **489**, 519–525.
- 10 L. Lignitto, S. E. LeBoeuf, H. Homer, S. W. Jiang, M. Askenazi, T. R. Karakousi, H. I. Pass, A. J. Bhutkar, A. Tsirigos, B. Ueberheide, V. I. Sayin, T. Papagiannakopoulos and M. Pagano, *Cell*, 2019, **178**, 316.
- 11 Y. Liu, F. C. Lang and C. Z. Yang, *Pharmacol. Ther.*, 2021, **217**, 107664.
- 12 D. M. Ren, N. F. Villeneuve, T. Jiang, T. D. Wu, A. Lau, H. A. Toppin and D. D. Zhang, *Proc. Natl. Acad. Sci. U. S. A.*, 2011, **108**, 1433–1438.
- 13 S. Vartanian, T. P. Ma, J. Lee, P. M. Haverly, D. S. Kirkpatrick, K. B. Yu and D. Stokoe, *Mol. Cell. Proteomics*, 2016, **15**, 1220–1231.
- 14 M. J. Bollong, H. Yun, L. Sherwood, A. K. Woods, L. L. Lairson and P. G. Schultz, *ACS Chem. Biol.*, 2015, **10**, 2193–2198.
- 15 A. Singh, S. Venkannagari, K. H. Oh, Y. Q. Zhang, J. M. Rohde, L. Liu, S. Nimmagadda, K. Sudini, K. R. Brimacombe, S. Gajghate, J. F. Ma, A. Wang, X. Xu, S. A. Shahane, M. G. Xia, J. Y. Woo, G. A. Mensah, Z. B. Wang, M. Ferrer, E. Gabrielson, Z. Y. Li, F. Rastinejad, M. Shen, M. B. Boxer and S. Biswal, *ACS Chem. Biol.*, 2016, **11**, 3214–3225.
- 16 S. Lee, M. J. Lim, M. H. Kim, C. H. Yu, Y. S. Yun, J. Ahn and J. Y. Song, *Free Radical Biol. Med.*, 2012, **53**, 807–816.
- 17 H. Liao, D. Zhu, M. Z. Bai, H. F. Chen, S. H. Yan, J. Yu, H. T. Zhu, W. X. Zheng and G. R. Fan, *Cancer Cell Int.*, 2020, **20**, 480.
- 18 D. Yu, Y. Liu, Y. Q. Zhou, V. Ruiz-Rodado, M. Larion, G. W. Xu and C. Z. Yang, *Proc. Natl. Acad. Sci. U. S. A.*, 2020, **117**, 9964–9972.
- 19 A. Cuadrado, A. I. Rojo, G. Wells, J. D. Hayes, S. P. Cousin, W. L. Rumsey, O. C. Attucks, S. Franklin, A. L. Levonen, T. W. Kensler and A. T. Dinkova-Kostova, *Nat. Rev. Drug Discovery*, 2019, **18**, 295–317.
- 20 D. Zhang, Z. Hou, K. E. Aldrich, L. Lockwood, A. L. Odom and K. T. Liby, *Mol. Cancer Ther.*, 2021, **20**, 1692–1701.
- 21 A. L. Odom, *Dalton Trans.*, 2005, 225–233, DOI: [10.1039/b415701j](https://doi.org/10.1039/b415701j).
- 22 A. L. Odom and T. J. McDaniel, *Acc. Chem. Res.*, 2015, **48**, 2822–2833.
- 23 C. S. Cao, Y. H. Shi and A. L. Odom, *J. Am. Chem. Soc.*, 2003, **125**, 2880–2881.
- 24 A. A. Dissanayake, R. J. Staples and A. L. Odom, *Adv. Synth. Catal.*, 2014, **356**, 1811–1822.
- 25 Y. H. Shi, C. Hall, J. T. Ciszewski, C. S. Cao and A. L. Odom, *Chem. Commun.*, 2003, 586–587, DOI: [10.1039/b212423h](https://doi.org/10.1039/b212423h).
- 26 M. H. Keylor, Z. L. Niemeyer, M. S. Sigman and K. L. Tan, *J. Am. Chem. Soc.*, 2017, **139**(31), 10613–10616, DOI: [10.1021/jacs.7b05409](https://doi.org/10.1021/jacs.7b05409).
- 27 G. D. Cuny, P. B. Yu, J. K. Laha, X. C. Xing, J. F. Liu, C. S. Lai, D. Y. Deng, C. Sachidanandan, K. D. Bloch and R. T. Peterson, *Bioorg. Med. Chem. Lett.*, 2008, **18**, 4388–4392.
- 28 A. R. Haight, A. E. Bailey, W. S. Baker, M. H. Cain, R. R. Copp, J. A. DeMattei, K. L. Ford, R. F. Henry, M. C. Hsu, R. F. Keyes, S. A. King, M. A. McLaughlin, L. M. Melcher, W. R. Nadler, P. A. Oliver, S. I. Parekh, H. H. Patel, L. S. Seif, M. A. Staeger, G. S. Wayne, S. J. Wittenberger and W. J. Zhang, *Org. Process Res. Dev.*, 2004, **8**, 897–902.
- 29 B. Harder, W. Tian, J. J. La Clair, A. C. Tan, A. Ooi, E. Chapman and D. D. Zhang, *Mol. Carcinog.*, 2017, **56**, 1493–1500.
- 30 C. Wiel, K. Le Gal, M. X. Ibrahim, C. A. Jahangir, M. Kashif, H. D. Yao, D. V. Ziegler, X. F. Xu, T. Ghosh, T. Mondal, C. Kanduri, P. Lindahl, V. I. Sayin and M. O. Bergo, *Cell*, 2019, **178**, 330.